sciendo

Polish Journal of Chemical Technology, 24, 3, 35—40, 10.2478/pjct-2022-0020

Synthesis, physicochemical studies, fluorescence behavior, and anticancer properties of transition metal complexes with the pyridyl ligand

Mohammad Azam*, Saud I. Al-Resayes

Department of Chemistry, College of Science, King Saud University, PO BOX 2455, Riyadh 11451, Saudi Arabia
**Corresponding author: e-mail: azam_res@yahoo.com*

A novel series of complexes with the formula [MLCl] [M = Co(II) (1), Ni(II) (2), Cu(II) (3), Zn(II) (4)] arising from Pyridyl ligand, N,N'-bis(1-(2-pyridyl)ethylidene)-2,2-dimethylpropane-1,3-diamine), ligand, L, was synthesized and investigated by elemental analyses, FT-IR, ^{1}H and ^{13}C NMR, Powder XRD, and thermal analyses. TGA analysis indicated that all complexes degraded in three different steps, while the PXRD examination showed well-defined sharp crystalline peaks for the complexes, indicating significant crystallinity. The antiproliferative activity of the ligand and its complexes were also evaluated *in vitro* against the HeLa (Human Cervical Cancer Cells) and HCT116 (Colon Cancer Cells) cell lines. The findings suggested complex **4** to be potential anticancer agent against these cell lines. In addition, ligand and its complexes also exhibited considerable emission properties.

Keywords: Pyridyl ligand; metal complexes; anticancer activity.

INTRODUCTION

Schiff base ligands are one of the most prominent nitrogen donor ligands in the field of inorganic chemistry due to their ability to chelate metal ions by donating lone pair of electrons. In addition, Schiff base ligands are easy to synthesize, stable, and adaptable[1–5]. Moreover, the Schiff base complexes are useful in a variety of contexts, including catalysis[6], photochromism[7, 8], nonlinear optics[9], magnetism[10], coordination chemistry[11], and materials science[12, 13].

Pyridyl ligands have gained a lot of attention among the various Schiff base ligands used in coordination chemistry because of their effective chelating properties and ability to develop distinct coordination architectures[12, 13]. The pyridyl functionality also improves electron delocalization and conformational rigidity after coordination to the metal ion, enhancing the luminescent, optical, catalytic, and medicinal properties of the complexes[14–18]. Over the years, cis-platin, a platinum-based drug, has been used to treat almost half of all cancer patients[19]. However, the use of cisplatin is restricted despite its therapeutic effectiveness in the treatment of cancer because it has serious toxic side effects such nephrotoxicity, neurotoxicity, hematologic toxicity, and ototoxicity. In addition, cisplatin has poor water solubility and can cause acquired resistance in a variety of cancer types[20].

Keeping in mind the benefits and downsides of platinum-based anticancer medications, researchers are therefore seeking for new potential anticancer medicines with high efficacy across a wide spectrum of tumours and low harmful side effects. Nitrogen-containing ligands and their metal complexes have drawn a lot of attention over the years due to their extensive biological applications, particularly when it comes to developing complexes with anticancer properties[21], which are attributed to electronic interactions between the metal center and the π-electrons in rings[22–23]. Therefore, taking into account the properties of nitrogen-containing ligands and their complexes, we study here a novel series of complexes of the first series of transition metal ions obtained from pyridyl ligand[12] and investigate their anticancer activity against HeLa (Human Cervical Cancer Cells) and HCT116 (Colon Cancer Cells) cancer cell lines. In addition, we have also reported their fluorescence behavior.

EXPERIMENTAL

Materials and methods

All of the chemicals, including 2,2-Dimethyl-1,3-propanediamine, 2-acetylpyridene, were procured from Sigma-Aldrich and utilized exactly as received. FT-IR spectra were collected on a Perkin Elmer 621 infrared spectrophotometer with KBr pallet. ^{1}H- and ^{13}C-NMR spectra in d_6-DMSO, as well as CHN, were obtained using a JEOL-400 spectrometer and an Elementar Varrio EL analyzer, respectively. The RF-6000 Spectro Fluorophotometer was used to obtain fluorescence spectra in methanol. The Powder XRD analysis with XRD pattern was performed using Cu Kα (λ = 1.54059 Å) radiation on Bruker D2 Phaser X-ray diffractometer.

Synthesis of Pyridyl ligand, (1E,1'E)-N,N'-(2,2-dimethylpropane-1,3-diyl)bis(1-(pyridin-2-yl)ethan-1-imine), L

A methanolic solution of 2,2-Dimethyl-1,3-propanediamine (100 mg, 0.98 mmol) was mixed with 2-acetylpyridene in a 1:2 molar proportion in the same solvent for 10 hours at ambient conditions, yielding crystalline solid after evaporation (Scheme 1). Unfortunately, we were unable to find a suitable crystal for diffraction.

Color, Yellow; Chemical Formula: $C_{19}H_{24}N_4$, Anal. Calc.: C, 73.99; H, 7.84; N, 18.17; Found: C, 73.79; H, 7.79; N, 18.10; ^{1}H NMR (d_6-DMSO, ppm): 8.58-7.38 (m, Ar-H, 8H), 3.39 (4H, N-C**H$_2$**), 2.26 (N=C–C**H$_3$**), 1.09 (6H, C–C**H$_3$**), ^{13}C-NMR (d_6-DMSO, ppm): 165.3 (-**C**=N), 148.1−157.0 (Ar-**C**), 36.5 (N-C−**C**H$_3$–CH$_2$−), 24.4 (-**C**H$_3$-C-**C**H$_3$), 60.1 (-CH$_3$-**C**-CH$_3$), IR (KBr, cm^{-1}): 1612

General procedure for the Synthesis of complexes

To the methanolic solution of ligand, L (50 mg, 0.162 mmol) was added metal salt in a 1:1 proportion followed by the vigorous stirring of the reaction mixture for 5 hours. Slight turbidity was obtained which was eliminated by filtration. The transparent and colored

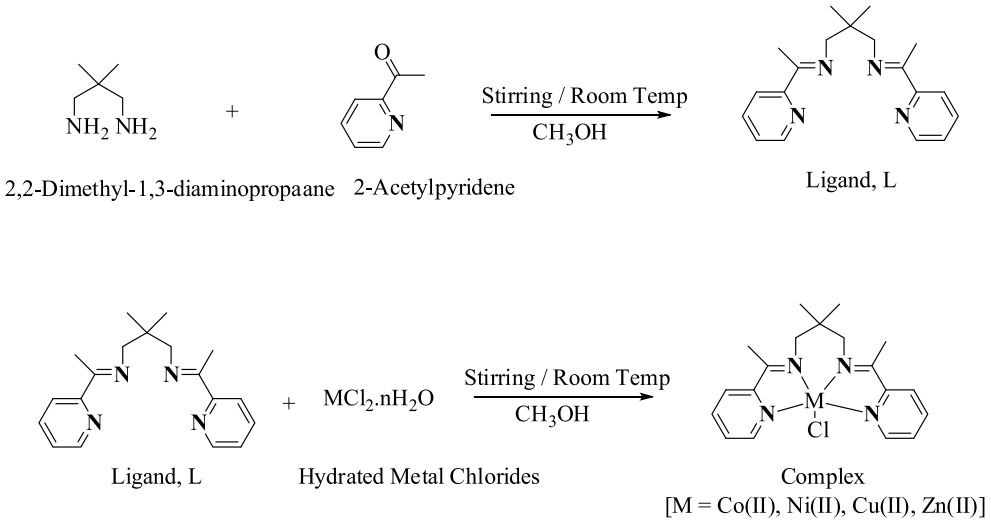

Scheme 1. Schematic representation of the synthesis of ligand and its complexes

solution was dried under vacuum and recrystallized in methanol to obtain an analytically pure compound.

Complex 1: Chemical Formula: $C_{19}H_{24}ClCoN_4$; Color: Brown, Anal. Cal: C, 56.65; H, 6.01; N, 13.91, Found: C, 56.61; H, 5.95; N, 13.84, IR (KBr, cm^{-1}): 1618

Complex 2: Chemical Formula: $C_{19}H_{24}ClN_4Ni$; Color: Greenish brown; Anal. Cal: C, 56.69; H, 6.01; N, 13.92; Found: C, 56.63; H, 5.96; N, 13.88; IR (KBr, cm^{-1}): 1613

Complex 3: Chemical Formula: $C_{19}H_{24}ClCuN_4$; Color, Blue; Anal. Cal: C, 56.01; H, 5.94; N, 13.75, Found: C, 55.97; H, 5.89; N, 13.71; IR (KBr, cm^{-1}): 1615

Complex 4: Chemical Formula: $C_{19}H_{24}ClN_4Zn$; Color: Yellow; Anal. Cal: C, 55.76; H, 5.91; N, 13.69; Found, C, 55.71; H, 5.85; N, 13.61; ^{1}H NMR (d_6-DMSO, ppm): 9.0-7.65 (m, Ar-H, 8H), 3.85 (4H, N-C**H$_2$**), 2.60 (N=C–C**H$_3$**), 1.20 (6H, C–C**H$_3$**), ^{13}C-NMR (d_6-DMSO, ppm): 165. 3 (-**C**=N), 156.7, 147.9, 136.2, 119.9 (Ar-**C**), 24.2 (N-C−**C**H$_3$–CH$_2$−), 59.9 (-**C**H$_2$-C-**C**H$_2$), 13.3 (-CH$_3$-**C**-CH$_3$), 35.2 (-CH$_2$-**C**-CH$_2$), IR (KBr, cm^{-1}): 1620

In vitro Cytotoxicity assay

The MTT assay was used to determine the cytotoxic activity of the ligand and its studied complexes. The MTT assay [(3-(4,5-dimethylthiazol-2-yl)-2,5-diphenyltetrazolium bromide), a yellow-colored water-soluble tetrazolium salt that cleaves the tetrazolium ring and converts it to a water-insoluble purple colored formazan when it interacts with living cells that contain a mitochondrial enzyme (succinate-dehydrogenase). The MTT [3-(4,5-dimethyl-2-thiaozolyl)-2,5-diphenyl-2H-tetrazolium bromide] assay was used to assess the anticancer activity of the investigated compounds in HeLa (Human Cervical Cancer Cells) and HCT116 (Colon Cancer Cells) cancer cell lines under different treatment conditions to detect mitochondrial dehydrogenase activity in living cells.

The pyridyl ligand and its complexes were tested *in vitro* against HeLa (Human Cervical Cancer Cells) and HCT116 (Colon Cancer Cells) cancer cell lines. Before the experiment, all the cancer cell lines were grown in Dulbecco's Modified Eagle Medium (DMEM) with 2 mM/L glutamine, 10% fetal bovine serum (FBS), 50 unit/ml penicillin, and 50 g/ml streptomycin in a 5% CO_2 and 95% air incubator at 37 °C[24–25]. The cells were seeded at a density of 1×10^4 cells/well in 96-well plates and cultured for 24 hours in 100 µL of DMEM at 37 °C in a 5% CO_2 atmosphere. Cells were treated in triplicate with increasing concentrations of the tested compounds dissolved in DMSO, ranging from 1–100 µM for 24 h. DMSO-treated cells were used as a control. As previously stated[19, 26–27], cell viability was determined using the tetrazolium dye, MTT 3-(4,5-dimethylthiazol-2-yl)-2,5-diphenyltetrazolium bromide. After 24 hours of incubation with the tested compound, the cells were given 10 µL liters of freshly prepared MTT (5 mM) solution and incubated for another 2 hours at 37 °C in 5% CO_2. The supernatants were then extracted, and 100 µL DMSO was pipetted into each well to solubilize the blue formazan products produced during MTT incubation[19, 26–27]. To assess cell viability, the absorbance of each well was measured using a UV–visible spectrophotometer at 630–550 nm, and the percent cell viability was calculated as follows:

percent viability = Test OD/Control OD x 100

The formula y = mx + b was used to measure IC50 values, where m and b indicate slope and intercept, respectively, using Microsoft Excel 2010.

RESULTS AND DISCUSSION

The Schiff base ligand L, which was made by condensing 2,2-dimethyl-1,3-diaminopropane and 2-acetylpyridine in a 1:2 molar ratio in methanolic medium is shown in Scheme 1. The isolated complexes [M(L)Cl] were produced in methanol by reacting the ligand, L, with metal ions [M= Co(II) (**1**), Ni(II) (**2**), Cu(II) (**3**), and Zn(II) (**4**)] in 1:1 molar ratio. All of the complexes investigated are non-ionic and stable at room temperature. Unfortunately, all of our efforts to get an appropriate crystal for single crystal X-ray crystallography remained unsuccessful.

The FT-IR spectra of the ligand and its studied complexes were analyzed, and the positions of various characteristic bands confirm the proposed structure for the ligand and its complexes. The most distinctive peak, 1612 cm^{-1}, owing to υ(C=N), confirms the formation of the studied ligand, L, which moved to 1613–1620 cm^{-1} after coordination to metal ions[12, 27–28]. The vibrations of the free ligand due to υ(Ar-CH) were detected at 3091 cm^{-1} [28, 29]. However, their location shifts to 3102–3110

cm^{-1}, once the metal is coordinated to the synthesized ligand[29, 30]. Furthermore, the aliphatic vibrations caused by the υ(C-H) stretching vibrations of -CH_2/CH_3 appeared at 2918–2960 cm^{-1} [12] [Supplementary Information Figure S1].

The ^{1}HNMR spectral findings of the pyridyl ligand and its zinc complex are mentioned in the Experimental Section, which support the recommended structure. Signals at 8.58–7.38 ppm are assigned to the pyridyl protons in the ligand, L. A proton adjacent to the nitrogen of the pyridyl moiety has a double doublet (1H, 8.08 ppm, J = 7.6 and 5.6 Hz), while the proton close to the side chain of the pyridyl moiety resonated at 8.1 ppm with coupling constant 8.0 Hz. The proton at the para position of the nitrogen of the pyridyl moiety appears at 7.78 ppm as a multiplier due to coupling and cross-coupling with neighboring protons. The proton linked by para proton and the proton next to the nitrogen of the pyridyl moiety appeared as a multiplet at 7.76 ppm. In addition, the chemical shifts due to the aliphatic protons corresponding to N=C–C**H$_3$**, N-C**H$_2$** and C–C**H$_3$** (6H, s) appear at 3.39 ppm, 2.26 ppm and 1.09 ppm, respectively. However, these positions are moved to 9.0–7.65 ppm (Ar-H, m, 8H) when coordinated to zinc ion, whereas the chemical shits for -H_2C–C**H$_3$**, N-C**H$_2$** at 1.20 ppm and 3.85 ppm, respectively [Figure 1 and 2].

The ^{13}C-NMR findings [Fig. 3] confirm the ^{1}H NMR observations, revealing the presence of a significant azomethine carbon signal at 165.3 ppm, as well as aromatic carbon signals at 148.1−157.0 ppm. Furthermore, the carbon signal owing to N-C−**C**H_3–**C**H_2−C−CH_2− and -**C**H_3-C-**C**H_3, -CH_3-**C**-CH_3 appear at 36.5, 70.5, 24.4

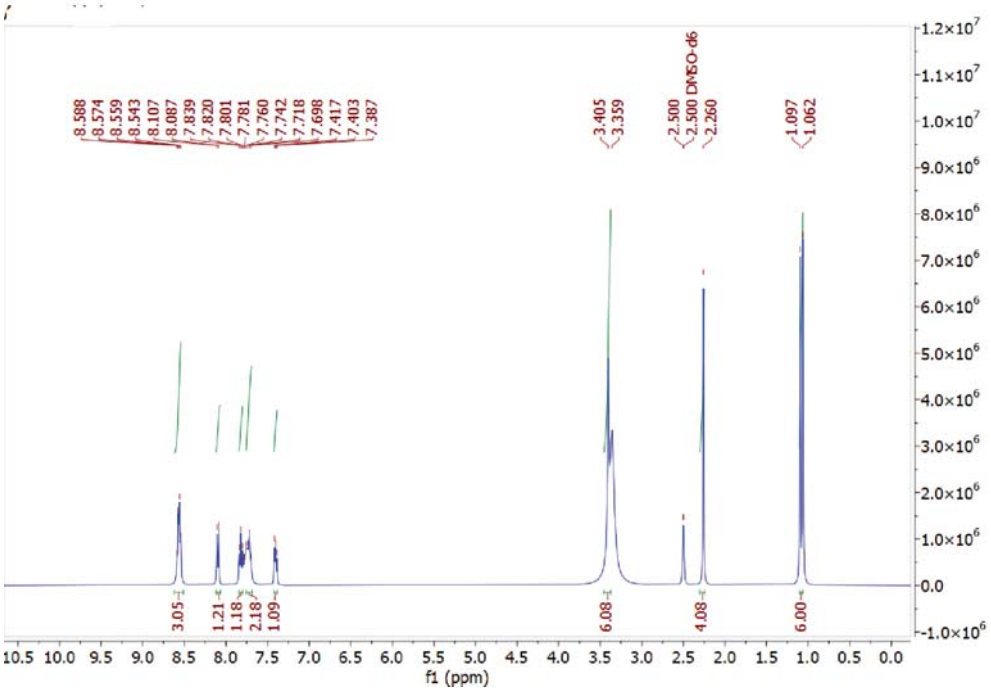

Figure 1. ^{1}H-NMR spectrum of ligand, L

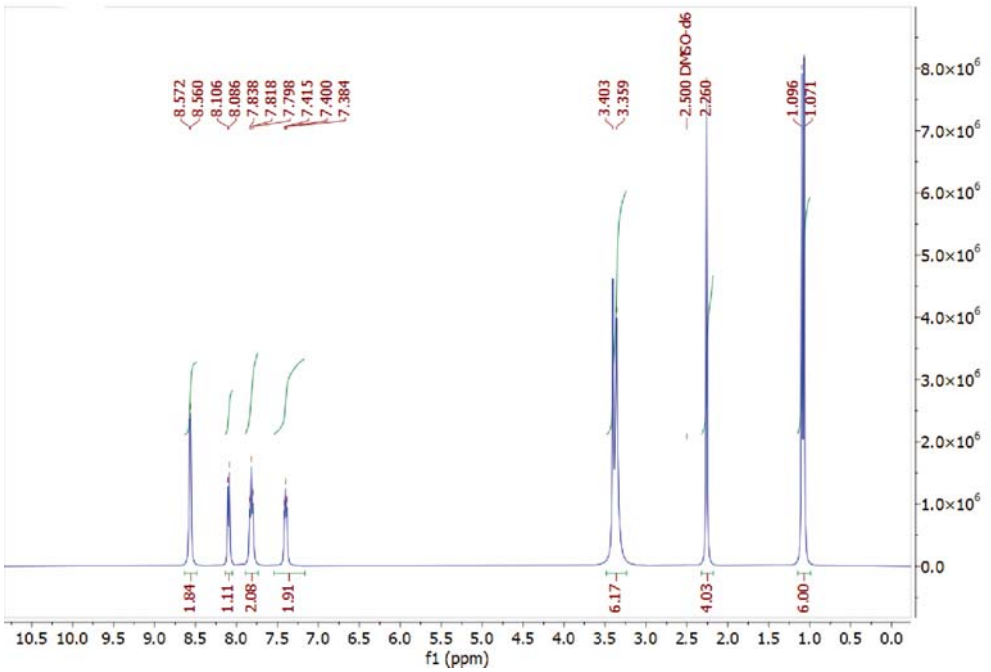

Figure 2. ^{1}H-NMR spectrum of complex 4

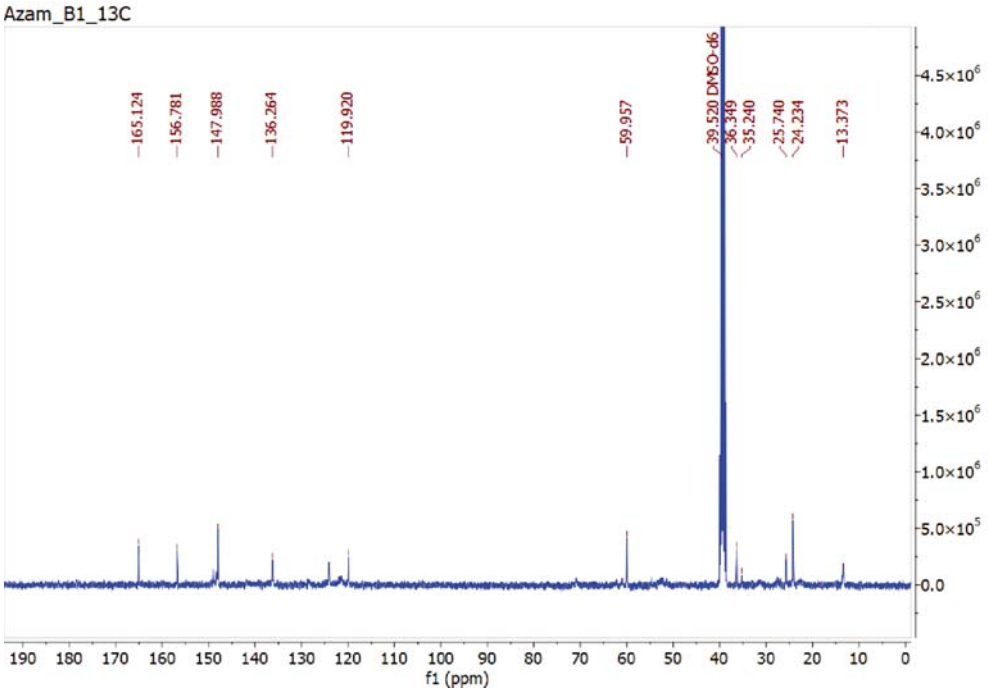

Figure 3. ^{13}C-NMR spectrum of complex 4

and 60.1 ppm, respectively [Supplementary Information Fig. S2]. However, the sites for carbon signals are shifted when metal ion is coordinated.

The Powder XRD analysis of the zinc complex was performed using X- Cu Kα (λ = 1.54059 Å) radiation powder X-ray powder diffraction for the studied complex was scanned at a wavelength of 1.5406 Å and 2θ range of 0°–90°. The results showed that the studied complexes had well-defined sharp crystalline peaks, indicating their strong crystallinity. Since all of the complexes have a similar structure, we only display the diffractogram of zinc complex [Fig 4]. The complex shows maximum reflection at 2θ = 23.45 and inter-planar distance at d = 3.79 Å, which was calculated by Bragg's equation n λ= 2dsin θ. Unit cell dimensions values a ≠ b ≠ c suggests Orthorhombic crystal structure with monoclinic space group. In addition, Scherrer's formula[21] was also used to measure the average crystallite size for the complex.

TGA was performed in an inert environment of nitrogen at a heating rate of 10 °C min^{-1} and a temperature range of 53–709 °C [Supplementary Information Fig. S3]. The degradation pattern was consistent across all complexes. Therefore, we've included only the TGA degradation of complex 4. The zinc complex causes a total weight loss of 68.41% in three stages. the first step occurs at about 53–70 °C, resulting in a slight weight loss of 7.42% due to one methanol molecule. The second stage of thermal decomposition, which occurred at temperatures between 150–200 °C, accounted for 21.58% of the total mass of the complex caused by the release of one acetyl moiety (C7H7NO). The third step, the largest weight loss stage, which happens at roughly 325 °C, accounts for 39.41% of the overall mass of the complex, equivalent to the whole remaining organic moiety. The production of ZnO as a final product (31.55%) is then indicated by a straight line.

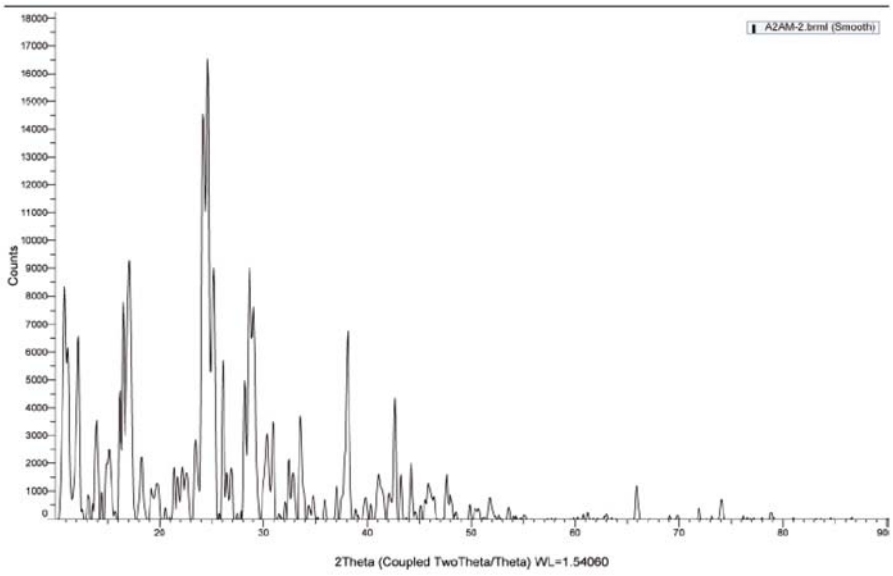

Figure 4. Powder X-Ray Diffractogram for complex 4

In-vitro Anticancer activity

MTT test was used to assess the antiproliferative activity of the ligand and its investigated compounds against HeLa (Human Cervical Cancer Cells) and HCT116 (Colon Cancer Cells). The cytotoxic behavior of the cancerous cell lines was investigated at various concentrations ranging from 1.0 μM to 50 μM for 24 h. However, at maximum concentration of 50 μM for cancer cell line HeLa, the ligand, complex 1, and 2 displayed 27.5%, 30.2%, and 31.7% cell viability, whereas the cell viability for cancer cell lines HCT116 for the ligand and complex 2 and 4 was observed 14.5%, 21.3%, and 25.8%. Table 1 shows the estimated IC50 values for both cell lines. Complex 4 With IC50 values of 20.9 μM and 17.5 μM showed strong anticancer activity against HeLa and HCT116 cell lines, respectively. Complex 3 also had significant anticancer activity against HeLa and HCT116 cell lines, with IC50 values of 22.7 μM and 21.5 μM, respectively. However, complex 2 was discovered to be moderately active against HeLa and HCT116, with an IC50 value of 23.2 μM and 23.8 μM, respectively. In contrast to complexes 2, 3, and 4, ligand and complex 1 displayed low anticancer activity, with IC50 values of 31.5 μM and 28.5 μM, and 25.7 μM and 24.1 μM, respectively against the HeLa and HCT116 cell lines. Overall, the findings indicate that all of the complexes have greater anticancer activity than the parent ligand. Complex 4 has, on the other hand, demonstrated potential anticancer activity in both cell lines.

Table 1. IC50 values for the cell lines

Compound	IC50 (μM)	
	HeLa	HCT116
L	31.5	28.5
1	25.7	24.1
2	23.2	23.8
3	22.7	21.5
4	20.9	17.5

Fluorescence properties

The fluorescence properties of the Schiff base ligand, L, and its complexes were reported in methanol at room temperature [Fig 5]. The emission peak appeared at 344 nm when the ligand was excited at 320 nm. The fluorescence activity of ligand is due to the intraligand π-π* transitions. All the complexes emitted a strong fluorescence emission band in the range of 346–351 nm when excited at 320 nm. However, complex 4 emits a broad emission peak. Thus, the emission peak of the free ligand and its metal complexes differed significantly, showing ligand-metal ion coordination.

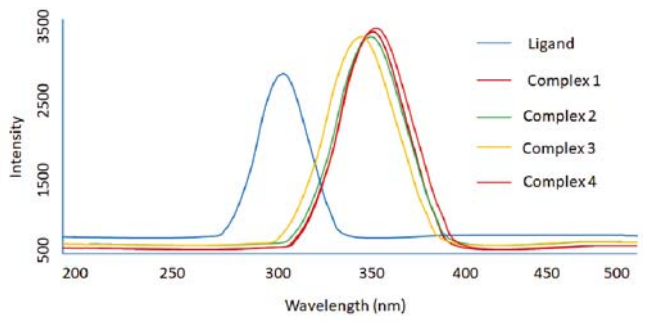

Figure 5. Fluorescence spectra of ligand and its complexes

CONCLUSION

A novel series of complexes with metal ions from the first transition series were produced from a pyridyl ligand and investigated using a variety of different spectroscopic techniques.

The investigated compounds showed significant ability to inhibit the growth of tumors when tested on Human cervical (HeLa) and colon cancer cells (HCT116). However, the findings revealed that complex 4 with the lowest IC50 has potential anticancer activity against all these cell lines.

ACKNOWLEDGMENTS

The authors acknowledge the financial support through Researchers Supporting Project number (RSP-2021/147), King Saud University, Riyadh, Saudi Arabia.

LITERATURE CITED

1. Cho, Y.I., Ward, M.L. & Rose, M.J. (2016). Substituent effects of N4 Schiff base ligands on the formation of fluoride--bridged dicobalt(II) complexes *via* B–F abstraction: structures and magnetism. *Dalton. Trans.* 45, 13466–13476. DOI: 10.1039/C6DT02104B.

2. Pradeepa, C.P. & Das, S.K. (2013). Coordination and supramolecular aspects of the metal complexes of chiral N-salicyl-*β*-amino alcohol Schiff base ligands: Towards understanding the roles of weak interactions in their catalytic reactions. *Coord. Chem. Rev.* 257, 1699–1715. DOI: 10.1016/j.ccr.2013.01.028.

3. Perlepe, P.S., Silva, L.C., Bekiari, V., Gagnon, K.J., Teat, S.J., Escuere, A. & Stamatatos,T.C. (2016). Structural diversity in Ni^{II} cluster chemistry: Ni_5, Ni_6, and $\{NiNa_2\}_n$ complexes bearing the Schiff-base ligand *N*-naphthalidene-2-amino-5-chlorobenzoic acid. *Dalton. Trans.* 45, 10256–10270. DOI: 10.1039/C6DT01162D

4. Roth, A., Spielberg, E.T. & Plass, W. (2007). Kit for Unsymmetric Dinucleating Double-Schiff-Base Ligands: Facile Access to a Versatile New Ligand System and Its First Heterobimetallic Copper−Zinc Complex. *Inorg. Chem.* 46, 4362–4364. DOI: 10.1021/ic070088i.

5. Vardhan, H., Mehta, A., Nathab, I. & Verpoort, F. (2015). Dynamic imine chemistry in metal–organic polyhedral. *RSC. Adv.* 5, 67011–67030. DOI.10.1039/C5RA10801B.

6. (a) Bhattacharjee, A., Halder, S., Ghosh, K., Rizzoli, C. & Roy, P. (2017). Mono-, tri- and polynuclear copper(II) complexes of Schiff-base ligands: synthesis, characterization and catalytic activity towards alcohol oxidation. *New. J. Chem.* 41, 5696–5706. DOI: 10.1039/C7NJ00846E. (b) Liu, X., González-Castro, A., Mutikainen, I., Pevec, A., Teat, S.J., Gamez, P., Costa, J.S., Bouwman, E. & Reedijk, J. (2016). Zinc and cadmium halide compounds with the tridentate ligand 2-(methylsulfanyl)-N-(pyridin-2-ylmethylidene)aniline showing yellow luminescence. *Polyhedron.* 110, 100–105. DOI: 10.1016/j.poly.2016.02.030. (c) O'Reilly, R.K., Gibson, V.C., White, A.J.P. & Williams, D.J. (2004). Five-coordinate iron(II) complexes bearing tridentate nitrogen donor ligands as catalysts for atom transfer radical polymerization. *Polyhedron.* 23, 2921–2928. DOI: 10.1016/j.poly.2004.09.001. (d) Bhaumik, P.K., Jana, S. & Chattopadhyay, S. (2012). Synthesis and characterization of square planar and square pyramidal copper(II) compounds with tridentate Schiff bases: Formation of a molecular zipper via H-bonding interaction. *Inorg. Chim. Acta.* 390, 167–177. DOI: 10.1016/j.ica.2012.04.004. (e) Gupta, K.C. & Sutar, A.K. (2008). Catalytic activities of Schiff base transition metal complexes. *Coord. Chem. Rev.* 252, 1420–1450. DOI: 10.1016/j.ccr.2007.09.005.

7. Al Rasbi, N.K. & Husband, J.J. (2016). Excitation and emission properties of Zn(II) Schiff base complex by combined

crystallographic, spectroscopic and DFT studies. *J. Photochem. Photobiol.* 314, 96–103. DOI: 10.1016/j.jphotochem.2015.08.007.

8. Hadjoudis, E. & Mavridis, I.M. (2014). Photochromism and thermochromism of Schiff bases in the solid state: structural aspects. *Chem. Soc. Rev.* 33, 579–588. DOI: 10.1039/B303644H

9. Yu, W., Jia, J., Gao, J., Han, L. & Li, Y. (2016). The preparation of a new type of ferrocene-based compounds with large conjugated system containing symmetrical aromatic vinyl with Schiff base moieties and the study of their third-order nonlinear optical properties. *Chem. Phys. Lett*. 661, 251–256. DOI: 10.1016/j.cplett.2016.04.096.

10. Biswas, R., Ida, Y., Baker, M.L., Biswas, S., Kar, P., Nojiri, H., Ishida, T. & Ghosh, A (2013). A New Family of Trinuclear Nickel(II) Complexes as Single-Molecule Magnets. *Chem. Eur. J.* 19, 3943–3953. DOI: 10.1002/chem.201202795.

11. Lee, J., Lee, H., Nayab, S. & Yoon, K.B. (2019). Synthesis, characterization and polymerisation studies of cadmium(II) complexes containing *N*,*N*′,*X*-tridentate *X*-substituted (*X* = *N*, *O*) 2-iminomethylpyridines. *Polyhedron.* 158, 432–440. DOI: 10.1016/j.poly.2018.11.033.

12. Azam, M., Wabaidur, S.M., Alam, M.J., Trzesowska--Kruszynska, A., Kruszynski, R., Alam, M., Al-Resayes, S.I., Dwivedi, S., Khan, M.R., Islam, M.S. & Albaqami, N.T.M. (2019). Synthesis, structural investigations and pharmacological properties of a new zinc complex with a N4-donor Schiff base incorporating 2-pyridyl ring. *Inorg. Chim. Acta.* 487, 97-106. DOI: 10.1016/j.ica.2018.12.009.

13. Satterfield, M. & Brodbelt, J.S. (2001). Relative Binding Energies of Gas-Phase Pyridyl Ligand/Metal Complexes by Energy-Variable Collisionally Activated Dissociation in a Quadrupole Ion Trap. *Inorg. Chem.* 40, 5393–5400. DOI: 10.1021/ic010356r.

14. Azam, M., Al-Resayes, S.I., Wabaidur, S.M., Trzesowska-Kruszynska, A., Kruszynski, R., Mohapatra, R.K. & Siddiqui, M.R.H. (2018). Cd(II) complex constructed from dipyridyl imine ligand: Design, synthesis and exploration of its photocatalytic degradation properties. *Inorg. Chim. Acta.* 471, 698–704. DOI: 10.1016/j.ica.2017.12.005.

15. (a) Scales, S.J., Zhang, H., Chapman, P.A., McRory, C.P., Derrah, E.J., Vogels, C.M., Saleh, M.T., Decken, A. & Westcott, S.A. (2004). Synthesis, characterization, and cytotoxicities of palladium(II) and platinum(II) complexes containing fluorinated pyridinecarboxaldimines. *Polyhedron.* 23, 2169–2176. DOI: 10.1016/j.poly.2004.06.013; (b) McDonnell, U., Kerchoffs, J.M.C.A., Castineiras, R.P.M., Hicks, M.R., Hotze, A.C.G., Hannon, M.J. & Rodger, A. (2008). Synthesis and cytotoxicity of dinuclear complexes containing ruthenium(II) bipyridyl units linked by a bis(pyridylimine) ligand. *Dalton. Trans*. 667–675. DOI: 10.1039/B711080D.

16. Samanta, B., Chakraborty, J., Choudhury, C.R., Dey, S.K., Dey, D.K., Batten, S.R., Jensen, P., Yap, G.P.A. & Mitra, S. (2007). Synthesis, characterisation and structural aspects of a new diorganotin(IV) complex with *N*′-(5-bromo-2-hydroxybenzylidene)benzoylhydrazone ligand. Struct. Chem. 18, 287–293. DOI: 10.1007/s11224-006-9133-y.

17. (a) Kettunen, M, Vedder, C., Brintzinger, H.-H., Mutikainen, I., Leskel€a, M. & Repo, T. (2005). Alternative Coordination Modes in Palladium(II)-Diimino-Bispyridine Complexes with an Axially Chiral Biphenyl Backbone. *Eur. J. Inorg. Chem*. 1081–1089. DOI: 10.1002/ejic.200400913; (b) Sibanyoni, J.M., Bagihalli, G.B. & Mapolie, S.F. (2012). Binuclear Pd-methyl complexes of *N,N*′-{1, *n*}-alkanediyl-*bis*(pyridinyl-2-methanimine) ligands (*n* = 5, 8, 9, 10 and 12): Evaluation as catalysts precursors for phenylacetylene polymerization. *J. Organomet. Chem.* 700, 93–102. DOI: 10.1016/j.jorganchem.2011.11.019; (c) Chen, R., Bacsa, J. & Mapolie, S.F. (2003). {*N*-alkyl-*N*-[pyridin-2-ylmethylene] amine}dichloro palladium(II) complexes: synthesis, crystal structures and evaluation of their catalytic activities for ethylene polymerization. *Polyhedron.* 22, 2855–2861. DOI: 10.1016/S0277-5387(03)00410-8.

18. Kumar, V., Manar, K.K., Gupta, A.N., Singh, V., Drew, M.G.B. & Singh, N. (2016). Impact of ferrocenyl and pyridyl groups attached to dithiocarbamate moieties on crystal structures and luminescent characteristics of group 12 metal complexes. *J. Organomet. Chem.* 820, 62–69. DOI: 10.1016/j.jorganchem.2016.08.007.

19. Pracharova, J., Vigueras, G., Novohradsky, V., Cutillas, N., Janiak, C., Kostrhunova, H., Kasparkova, J., Ruiz, J. & Brabec, V. (2018). Exploring the Effect of Polypyridyl Ligands on the Anticancer Activity of Phosphorescent Iridium(III) Complexes: From Proteosynthesis Inhibitors to Photodynamic Therapy Agents. *Chem. Eur. J.* 24, 4607–4619. DOI: 10.1002/chem.201705362.

20. Al-Resayes, S.I., Azam, M., Trzesowska-Kruszynska, A., Kruszynski, R., Soliman, S.M., Mohapatra, R.K. & Khan, Z. (2020). Structural and Theoretical Investigations, Hirshfeld Surface Analyses, and Cytotoxicity of a Naphthalene-Based Chiral Compound. *ACS. Omega*. 5, 27227–27234. DOI: 10.1021/acsomega.0c03376.

21. Li, J.J., Guo, L., Tian, Z., Tian, M., Zhang, S., Xu, K., Qian, Y. & Liu, Z. (2017). Novel half-sandwich iridium(III) imino-pyridyl complexes showing remarkable *in vitro* anticancer activity. *Dalton. Trans.* 46, 15520–15534. DOI: 10.1039/C7DT03265J.

22. Stepanenko, I.N., Casini, A., Edafe, F., Novak, M.S., Arion, V.B., Dyson, P.J., Jakupec, M.A. & Kepple, B.K. (2011). Conjugation of Organoruthenium(II) 3-(1*H*-Benzimidazol-2-yl) pyrazolo[3,4-*b*]pyridines and Indolo[3,2-*d*]benzazepines to Recombinant Human Serum Albumin: a Strategy To Enhance Cytotoxicity in Cancer Cells. *Inorg. Chem.* 50, 12669–12679. DOI: 10.1021/ic201801e.

23. Sava, G., Bergamoa, A. & Dyson, P.J. (2011). Metal-based antitumour drugs in the post-genomic era: what comes next. *Dalton. Trans*. 40, 9069–9075. DOI: 10.1039/C1DT10522A.

24. Mallela, R., Konakanchi, R., Guda, R., Munirathinam, N., Gandamalla, D., Yellu, N.R. & Kotha, L.R. (2018). Zn(II), Cd(II) and Hg(II) metal complexes of 2-aminonicotinaldehyde: Synthesis, crystal structure, biological evaluation and molecular docking study. *Inorg. Chim. Acta,* 469, 66–75. DOI: 10.1016/j.ica.2017.08.042.

25. Kritsanawong, S., Innajak, S., Imoto, M. & Watanapokasin, R. (2016). Antiproliferative and apoptosis induction of α-mangostin in T47D breast cancer cells. *Int. J. Oncology* 48, 2155–2165. DOI: 10.3892/ijo.2016.3399.

26. Huang, Y.C., Haribabu, J., Chien, C.M., Sabapathi, G., Chou, C.K., Karvembu, R., Venuvanalingam, P., Ching, W.M., Tsai, M.L. & Hsu, S.C.N. (2019). Half-sandwich Ru(η^6-*p*-cymene) complexes featuring pyrazole appended ligands: Synthesis, DNA binding and *in vitro* cytotoxicity. *J. Inorg. Biochem.* 194, 74–84. DOI: 10.1016/j.jinorgbio.2019.02.012.

27. Azam, M,. Wabaidur, S.M., Alam, M., Khan, Z., Alanazi, I.O., Al-Resayes, S.I., Moon, I.S. & Rajendra. (2021). Synthesis, characterization, cytotoxicity, and molecular docking studies of ampyrone-based transition metal complexes. *Trans. Met. Chem.* 46, 65–71. DOI: 10.1007/s11243-020-00422-8.

28. Shakir, M., Azam, M., Azim, Y., Parveen, S. & A.U. Khan, A.U. (2007). Synthesis and physico-chemical studies on complexes of 1,2-diaminophenyl-*N*,*N*′-bis-(2-pyridinecarboxaldimine), (L): A spectroscopic approach on binding studies of DNA with the copper complex. *Polyhedron***.** 26, 5513–5518. DOI: 10.1016/j.poly.2007.08.032.

29. Nakamoto, K. (1986). Infrared and Raman Spectra of Inorganic and Coordination Compounds. Fourth ed. New York, Wiley Interscience. (1986).

30. Bre´fuel, N., Vang, I., Shova, S., Dahan, F., Costes, J.-P. & Tuchagues¸ J.-P. (2007). Fe^{II} Spin crossover materials based on dissymmetrical N_4 Schiff bases including 2-pyridyl and 2R--imidazol-4-yl rings: Synthesis, crystal structure and magnetic and Mössbauer properties. *Polyhedron* 26, 1745–1757. DOI: 10.1016/j.poly.2006.12.017.